



Published in final edited form as:

Gastroenterology. 2010 March ; 138(3): 993–1002.e1. doi:10.1053/j.gastro.2009.11.009.

An *Msh2* Conditional Knockout Mouse for Studying Intestinal Cancer and Testing Anti-cancer Agents

Melanie H. Kucherlapati^{1,†}, KyeRyoung Lee^{2,†}, Andrew A. Nguyen^{1,†}, Alan B. Clark³, Harry Hou Jr.², Andrew Rosulek¹, Hua Li⁶, Kan Yang⁴, Kunhua Fan⁴, Martin Lipkin⁴, Roderick T. Bronson⁵, Linda Jelicks⁶, Thomas A. Kunkel³, Raju Kucherlapati¹, and Winfried Edelmann²

¹Department of Medicine, Brigham and Women's Hospital, Harvard Medical School, Boston, MA 02115

²Department of Cell Biology, Albert Einstein College of Medicine, Bronx, NY 10461

³Laboratory of Molecular Genetics, and Laboratory of Structural Biology, National Institute of Environmental Health Sciences, NIH, DHHS, Research Triangle Park, NC 27709

⁴Strang Cancer Research Laboratory, Department of Medicine (Gastroenterology), Weill Medical Center of Cornell University, New York, NY 10021

⁵Rodent Histopathology Core, Harvard Medical School, Boston, MA 02115 and Department of Pathology, Tufts University Schools of Medicine and Veterinary Medicine, Boston, MA 02111

⁶Department of Physiology and Biophysics, Albert Einstein College of Medicine, Bronx, NY, 10461

Abstract

Background & Aims—Mutations in the DNA mismatch repair (MMR) gene *MSH2* cause Lynch Syndromes I & II, and sporadic colorectal cancers (CRCs). *Msh2*^{null} mice predominantly develop lymphoma and do not accurately recapitulate the CRC phenotype.

Methods—We generated and examined mice with a conditional *Msh2* disruption (*Msh2*^{LoxP}), permitting tissue-specific gene inactivation. *ECMsh2*^{LoxP/LoxP} mice carried an *EIIa-Cre* transgene and *VCMsh2*^{LoxP/LoxP} mice carried a *Villin-Cre* transgene. We combined the *VCMsh2*^{LoxP} allele

Correspondence: Melanie Kucherlapati, PhD., Department of Medicine/Division of Genetics, Brigham and Women's Hospital, Harvard Medical School, Boston, MA 02115. mkucherlapati@partners.org or Winfried Edelmann, PhD., Department of Cell Biology, Albert Einstein College of Medicine, 1301 Morris Park Ave., Bronx, NY, 10461. edelmann@aecom.yu.edu.

[†] These authors contributed equally to this work.

Disclosures: N/A

Transcript profiling: N/A

Writing assistance: N/A

Study Concept and design: MHK, KL, RK, WE

Acquisition of data: MHK, KL, AN, AC, HH, AR, KY, KF, ML, RB, LJ

Analysis and interpretation of data: MHK, KL, AC, KY, RB, LJ, TK, RK, WE

Drafting of the manuscript: MHK, RK, WE

Critical revision of manuscript, important intellectual content: MHK, RB, KY, RK, WE

Statistical analysis: KL, KF, KY, WE

Obtained funding: ML, TK, RK, WE

Technical or material support: MHK, KL, AN, AC, HH, AR, KY, KF, ML, RB, LJ

Study supervisor: MHK, KL, RK, WE

Publisher's Disclaimer: This is a PDF file of an unedited manuscript that has been accepted for publication. As a service to our customers we are providing this early version of the manuscript. The manuscript will undergo copyediting, typesetting, and review of the resulting proof before it is published in its final citable form. Please note that during the production process errors may be discovered which could affect the content, and all legal disclaimers that apply to the journal pertain.

with either *Msh2*^{Δ7null} (*VCMsh2*^{LoxP/null}) or *Msh2*^{G674D} mutations (*VCMsh2*^{LoxP/G674D}) to create allelic phase mutants. These mice were given cisplatin, or 5-fluorouracil/leucovorin and oxaliplatin (FOLFOX) and their tumors were measured by magnetic resonance imaging.

Results—Embryonic fibroblasts from *ECMsh2*^{LoxP/LoxP} mice do not express MSH2 and are MMR-deficient. Reverse transcription, PCR, and immunohistochemistry from *VCMsh2*^{LoxP/LoxP} mice demonstrated specific loss of *Msh2* mRNA and protein from epithelial cells of the intestinal tract. Microsatellite instability (MSI) was observed in all *VCMsh2* strains and limited to the intestinal mucosa. Resulting adenomas and adenocarcinomas had somatic *Apc* truncation mutations. *VCMsh2*^{LoxP/LoxP} mice did not develop lymphoma. Comparison of allelic phase tumors revealed significant differences in multiplicity and size. When treated with cisplatin or FOLFOX, tumor size was reduced in *VCMsh2*^{LoxP/G674D} but not *VCMsh2*^{LoxP/null} tumors. The apoptotic response to FOLFOX was partially sustained in the intestinal mucosa of *VCMsh2*^{LoxP/G674D} animals.

Conclusion—*Msh2*^{LoxP/LoxP} mice in combination with appropriate Cre recombinase transgenes have excellent potential for preclinical modeling of Lynch Syndrome, MMR deficient tumors of other tissue types, and use in drug development.

Keywords

MMR; *Msh2*; mouse; tumorigenesis; chemotherapy

Background & Aims

Approximately 150,000 new cases of colorectal cancer (CRC) are diagnosed per year in the United States. More than 50,000 patients die from it yearly. Generally classified into familial predisposition syndromes and sporadic cancers, several critical genes involved in both have been identified. Familial adenomatous polyposis (FAP) is caused by mutations in the *APC* gene. Lynch Syndromes I & II are caused by mutations in the Mismatch Repair (MMR) genes. *MSH2* was found to be one of the most commonly mutated MMR genes¹⁻³. *Msh2* is necessary for repair of base-base as well as insertional deletion mismatches and its absence results in increased mutation levels. Mice lacking MSH2 have a tumor disposition phenotype.

To develop mouse models for Lynch Syndrome three *Msh2*^{null} knockout mouse lines have been generated, two by targeted disruption of *Msh2* exon 12^{4, 5} and one by disruption of exon 7⁶. Homozygous mutant mice of all three *Msh2*^{null} knockouts are MMR-deficient and display a highly increased predisposition to lymphoma. A proportion of older animals also develop intestinal neoplasms that are associated with *Apc* inactivation⁷. However, the predominance of the lymphoma phenotype has limited the use of these animals as preclinical models.

We report a novel conditional knockout mouse model for the tissue-specific inactivation of *Msh2* (*Msh2*^{LoxP}). In this model, MMR can be inactivated by *Cre-LoxP*-mediated inactivation of *Msh2* in different tissues by the expression of various *Cre-recombinase* transgenes. To constitutively inactivate MMR similar to *Msh2*^{null} knockout mice we mated *Msh2*^{LoxP} mice with *EIIa-Cre* recombinase transgenic mice (termed *ECMsh2*^{LoxP}). To specifically inactivate MMR in the intestinal mucosa we combined the *Msh2*^{LoxP} allele with the *Villin-Cre* transgene (*VCMsh2*^{LoxP}). *ECMsh2*^{LoxP/LoxP} mice display complete MMR deficiency and have a cancer phenotype similar to *Msh2*^{null} knockout mice. In contrast, in *VCMsh2*^{LoxP/LoxP} mice MMR deficiency is limited to the intestinal epithelium and the mice develop exclusively intestinal neoplasms. These data show that *Msh2*^{LoxP} mice in

combination with specific *Cre* recombinase transgenes allow the tissue-specific inactivation of MMR and the development of suitable mouse models for Lynch Syndrome.

We also demonstrate that it is possible to study allelic effects of different *Msh2* mutations on intestinal tumorigenesis in *VCMsh2^{LoxP}* mice by combining the *Msh2^{LoxP}* allele with either a Lynch Syndrome related missense mutation (*Msh2^{G674D}*) or an *Msh2^{Δ7null}* mutation (*Msh2^{null}*). Tumors from these allelic phase mutants have also been tested for their response to two chemotherapeutic regimens, cisplatin and FOLFOX, and their growth recorded by Magnetic Resonance Imaging (MRI). Although some tumors in *VCMsh2^{LoxP/null}* mice were responsive to the two drugs, the majority were resistant to both chemotherapies. In contrast, almost all *VCMsh2^{LoxP/G674D}* tumors were found to generally respond well to cisplatin and FOLFOX. The differences in responsiveness of tumors correlated with the absence of a significant DNA damage response in *VCMsh2^{LoxP/null}* mice, and partial retention of this response in *VCMsh2^{LoxP/G674D}* mice.

Methods

Generation of *Msh2^{LoxP}* Mice

The targeting vector for the *Msh2^{LoxP}* mouse was made by recombinogenic methods^{8, 9}. An *Msh2* genomic fragment spanning exon 10 through intron 18 was PCR amplified from BAC clone 183K13 (RP-22 library) and subcloned. A *LoxP* site was introduced into *Msh2* intron 12-13 followed by introduction of a *LoxP-FRT-PGKneo^r-FRT* selection cassette into *Msh2* intron 11-12. The vector was linearized and transfected into WW6 ES cells¹⁰. Male chimeric mice were generated and bred to C57BL/6J females to generate *Msh2neo^{LoxP-FRT neo/+}* F1 offspring. The *PGKneo^r* cassette was subsequently deleted *in vivo* by crossing *Msh2neo^{LoxP-FRT neo/+}* heterozygotes to *FLP- deleter* mice¹¹. Offspring from these crosses were genotyped by PCR, Southern Blot and sequence analyses (data not shown), to confirm the integrity of the *Msh2^{LoxP}* allele. All procedures were in accordance with Institutional Animal Care and Use Committee Protocols.

Generation of *Msh2^{LoxP} Cre Recombinase Transgenic Mouse Lines*

Msh2^{LoxP/+} mice were crossed with *EIIa-Cre recombinase* transgenic animals to generate *ECMsh2^{LoxP/+}*¹². Heterozygotes were intercrossed to generate *ECMsh2^{LoxP/LoxP}* mice.

Msh2^{LoxP/+} mice were mated with *B6;D2-Tg(Vil-Cre)* to create *VCMsh2^{LoxP/+}* mice, then intercrossed to create *VCMsh2^{LoxP/LoxP}* mice¹³. *VCMsh2^{LoxP/+}* mice were also mated to animals carrying the *Msh2^{Δ7}* knockout allele (termed *Msh2^{null}*)⁶ and the *Msh2^{G674D}* knock-in allele. Offspring with one floxed *Msh2* allele and one mutant allele, *VCMsh2^{LoxP/null}* or *VCMsh2^{LoxP/G674D}* respectively were obtained.

PCR Genotyping *Msh2^{LoxP}* mice

Tail DNA was isolated using the DNAeasy kit (Qiagen, Valencia, CA) from ten day old mice. PCR primers used for genotyping were 184F (TACTGATGCGGGTTGAAGG), 184R (AACCAGAGCCTCAACTAGC), and 165R (GGCAAACCTCCTCAAATCACG). Cycling conditions will be given upon request.

MMR analysis in *ECMsh2^{LoxP/LoxP}* MEF cell lines

Cytosolic extracts were prepared from MEF cells as described in Thomas et al.¹⁴. A heteroduplex G-G substrate was prepared and DNA repair reactions were performed as previously described^{14, 15}.

Western Blotting and Immunohistochemistry

MEF cell extracts were separated by SDS-PAGE and blotted onto Polyvinylidene fluoride membranes and probed with rabbit anti mouse MSH2 polyclonal antibody (MSH2 N-20:sc494, Santa Cruz, CA), an *Msh6* monoclonal antibody (BD Biosciences, Franklin, USA) or a GADPH monoclonal antibody (Ambion for GADPH, Austin, TX).

For immunohistochemical analysis (IHC), monoclonal antibodies directed against *Msh2* (N-20:sc494, Santa Cruz) and *Apc* (GTX15270, GeneTex, Inc.) were used.

Generation of Kaplan-Meier Survival Plots

Prism 3.0 software (Graphpad) was used to calculate percent survival of animals.

Histopathologic analysis

Mice were euthanized and the GI tract was removed, opened longitudinally, and fixed in 10% neutral-buffered formalin or Bouins solution. The number of tumors and their location was recorded under a dissecting microscope. For histological analysis, tumors were embedded in paraffin, sectioned to 5 μ m and stained with hematoxylin and eosin. Relative tumor size was measured using a Vernier Caliper with fine adjustment.

MSI Analysis

Genomic DNAs from tail, spleen and flat mucosa were subjected to PCR amplification using a dilution assay as previously described¹⁶. We screened for instability using a dinucleotide repeat marker, *D17Mit123*¹⁷. In intestinal tumors two dinucleotide markers were studied in undiluted DNA, *D7Mit91* and *TG27*. PCR products were separated on denaturing 6% polyacrylamide gels and autoradiographed for analysis.

Apc Truncation Mutations

The analysis of truncation mutations to the *Apc* gene was performed as described earlier¹⁸.

Drug Treatment

VCMsh2^{LoxP/null} and *VCMsh2^{LoxP/G674D}* animals were divided into 3 groups. The first group received an intraperitoneal injection (i.p.) with cisplatin (20 mg/kg body weight), five times every second day with a total dose of 100 mg/kg body weight. The second group received an i.p. injection with FOLFOX (5-fluorouracil/leucovorin, five sequential days (20 mg and 10 mg/kg body weight respectively); Oxaliplatin (1 mg/kg body weight) was injected i.p. once. The third group was a control group injected i.p. with Phosphate Buffered Saline (PBS) five times every second day. All drugs were purchased from Sigma-Aldrich Corp. (St. Louis, MO).

Magnetic Resonance Imaging (MRI) & 3-D Reconstitution of Images

Tumor sizes were measured before and after treatment by *in vivo* MRI imaging. Animals were positioned in a 40 mm “bird cage” MRI coil in a 9.4 T GE Omega vertical bore imaging system. A 51.2 mm field of view with a 256 \times 256 pixel image matrix was used. Image slices were 1 mm thick with no gap between slices. Series of routine spinecho images along all three planes were acquired to reconstruct 3D images of the mouse. Typical parameters for GI tract studies were used with echo time of 30 ms, repetition time of 400 ms, and signal averaging 4 scans. Typically 24 images were acquired along each plane. Image data was analyzed using MATLAB based software. 3D reconstructions of the digestive tract were created using Amira 3.1 software.

DNA Damage Response

TUNEL assays were conducted on intestinal and spleen tissue from *VCMsh2^{LoxP/null}* and *VCMsh2^{LoxP/G674D}* mice, (Promega DeadEnd (TM) Fluorometric TUNEL System).

Results

The Generation of *Msh2^{LoxP}* Mice, *ECMsh2^{LoxP/LoxP}* Cell Lines, and MMR Measurement

We have generated a conditional knockout mouse line for *Msh2* by flanking exon 12, encoding a portion of the essential ATPase domain of MSH2, with LoxP sites (Fig. 1A, B, & C). To constitutively delete exon 12, *Msh2^{LoxP/+}* were mated with *EIIa-Cre* recombinase mice. In these mice, the *Msh2^{LoxP}* allele was transmitted in a normal Mendelian ratio, and *ECMsh2^{LoxP/LoxP}* mice obtained upon heterozygote intercrosses also developed normally. Western blot analysis of *ECMsh2^{LoxP/LoxP}* MEFs revealed that deletion of exon 12 resulted in the complete loss of MSH2 protein, and also reduced levels of MSH6 protein (Fig. 2D).

To investigate the effect of *Msh2* exon 12 deletion on MMR, cell extracts from two MEF lines (*ECMsh2^{LoxP/LoxP}* lines 1 and 2) were screened for their ability to repair a G-G mismatch from a 3' nick. Neither extract repaired this single base mismatch. Repair deficiencies in both *ECMsh2^{LoxP/LoxP}* cell extracts were similar to repair deficiencies in an *Exo1^{Δ6/Δ6}* (exon 6 deletion) extract, previously found defective for repair of single base mismatches¹⁹. The MMR defect in both *ECMsh2^{LoxP/LoxP}* extracts was complemented by adding *Exo1^{Δ6/Δ6}* extract, demonstrating that it was caused by the specific loss of MSH2. After complementation of the *ECMsh2^{LoxP/LoxP}* extracts by the *Exo1^{Δ6/Δ6}* extract, a reduction in the blue/white plaque color ratios was found, demonstrating that repair activity in the complemented extracts is directed to the nicked strand, indicating strand-specific MMR (Fig.2B).

Inactivation of *Msh2* by *Villin-Cre* in *VCMsh2^{LoxP}* Mice

To inactivate *Msh2* in the intestinal mucosa, *Msh2^{LoxP/+}* animals were intercrossed with *Villin-Cre* transgenic mice¹³. *Msh2* inactivation was confirmed by PCR (Fig. 2A) and RT-PCR (Fig. 2F). Genomic DNA isolated from kidney, heart and spleen displayed either minimal or no exon 12 deletion.

MSH2 expression was examined by immunohistochemistry (Fig. 2E). It was detectable in the cytoplasm and nucleus of epithelial cells in wild-type mice, but was absent in the intestinal mucosa of *VCMsh2^{LoxP/LoxP}* mice.

To study the effect of exon 12 deletion on MMR *in vivo* we analyzed MSI in different tissues of *VCMsh2^{LoxP/LoxP}* mice (Fig. 2C). At the *DI7Mit123* locus only 5 of 77 (6.5%) alleles were unstable in genomic tail DNA of *VCMsh2^{LoxP/LoxP}* mice and 6 of 82 (7.3%) were unstable in spleen genomic DNA which is comparable to the levels of MSI in wild-type mice for this marker¹⁹. However, epithelial cells in the intestinal mucosa of *VCMsh2^{LoxP/LoxP}* mice displayed a significant increase in MSI with 20 of 96 unstable alleles (20.8%) indicating that the MMR-deficiency is highly restricted to the intestinal epithelium in *VCMsh2^{LoxP/LoxP}* mice.

Survival and Tumor Development in *ECMsh2^{LoxP/LoxP}* and *VCMsh2^{LoxP/LoxP}* Mice

Both *ECMsh2^{LoxP/LoxP}* and *VCMsh2^{LoxP/LoxP}* mice were viable and fertile. However, a significant difference in survival was observed between the two mouse lines ($p < 0.0001$) (Fig. 3B). The median survival for *VCMsh2^{LoxP/LoxP}* animals was 12 months and all animals expired at 17 months. In contrast, *ECMsh2^{LoxP/LoxP}* mice had a reduced median survival of 6 months and all animals died by 11 months similar to *Msh2^{null/null}* knockout mice⁴⁻⁶.

The analysis of several moribund *ECMsh2^{LoxP/LoxP}* mice at 6 to 7 months of age revealed a high incidence of lymphoma (67% of animals) and a lower incidence of small intestinal tumors (33% of animals) indicating that the cancer predisposition phenotype in *ECMsh2^{LoxP/LoxP}* mice is comparable to that of *Msh2^{null/null}* knockout mice^{4, 5} (Table 1).

In contrast, the cancer phenotype differed significantly between *VCMsh2^{LoxP/LoxP}* mice and *Msh2^{null/null}* knockout mice. A cohort of *VCMsh2^{LoxP/LoxP}* mice (n=18) was sacrificed at 9.0±1.1 months of age and analyzed for the presence of tumors. 89% of *VCMsh2^{LoxP/LoxP}* mice developed tumors in the small intestine at this age with a tumor multiplicity of 1.6±0.3 (Table 1). Histopathological analysis of 14 tumors showed that 50% were at the adenomas and the other 50% were highly invasive adenocarcinomas (Fig. 3A, C, D, & E). None of these animals developed lymphoma and only one in 150 *VCMsh2^{LoxP/LoxP}* mice developed lymphoma after 12 months of life. *VCMsh2^{LoxP/+}* mice (n=15) at 11.3±1.8 months of age developed no tumors and 1 of 17 (6%) wild-type mice at 14.2±2.7 months of age developed an intestinal tumor (Table 1). We also analyzed the MSI status in the genomic DNA of the intestinal tumors in *VCMsh2^{LoxP/LoxP}* mice at two dinucleotide markers. We found that at the *D7Mit123* marker 7 of 12 (58%) tumors tested were unstable, while at the *TG* marker¹⁶ 11 of 12 (92%) tumors were unstable. All tumors showed MSI of at least one of the two markers tested.

Apc is Mutated in *VCMsh2^{LoxP/LoxP}* GI Tumors

Immunohistochemistry of intestinal tumors from *VCMsh2^{LoxP/LoxP}* mice were negative for *Apc* antibody staining (Fig. 3F).

Truncation mutations in *VCMsh2^{LoxP/LoxP}* GI tumors were found by IVTT analysis indicating somatic mutations to both *Apc* alleles may have occurred for tumor initiation (Table 2). Twenty out of thirty-one (64.5%) *VCMsh2^{LoxP/LoxP}* tumors screened were positive. Ten fragments were cloned and sequenced. Mutation types included mono and di-nucleotide deletions and C to T transitions leading to the formation of stop codons. These mutations are consistent with the types of mutations caused by loss of **MMR** function¹⁸.

Allelic Phasing of Intestinal Tumor Development in *VCMsh2^{LoxP}* Mice

The *Msh2^{LoxP}* allele provided an opportunity to examine the impact of different *Msh2* mutations on intestinal tumor development. We generated *VCMsh2^{LoxP}* mice that carried the *Msh2^{LoxP}* allele in combination with either an *Msh2^{null}* (12) allele or the *Msh2^{G674D}* allele previously found in an HNPCC patient²⁰ (Supplemental data). Deletion of exon 12 in the *Msh2^{LoxP}* allele by *Villin-Cre* expression leads to intestinal epithelial cells containing two *Msh2^{null}* alleles (that express no MSH2) in *VCMsh2^{LoxP/null}* mice or one *Msh2^{null}* and one *Msh2^{G674D}* allele (that only express MSH2^{G674D}) in *VCMsh2^{LoxP/G674D}* mice. The analysis of tumorigenesis in these mice revealed remarkable differences (Fig. 4 A & B). Mice of both lines displayed a strong predisposition to intestinal cancers. However, the tumor onset was delayed in *VCMsh2^{LoxP/G674D}* mice as compared to *VCMsh2^{LoxP/null}* mice. In *VCMsh2^{LoxP/null}* mice intestinal tumors were found beginning at 6 months of age and 50% of animals carried intestinal tumors at 10 months of age. In contrast, intestinal tumors were first detected in *VCMsh2^{LoxP/G674D}* mice at 10 months of age and 50% of animals carried tumors at 13 months of age (p<0.0001). In addition, the tumor number and size differed significantly between the *VCMsh2^{LoxP/null}* and *VCMsh2^{LoxP/G674D}* allelic phase mutants. While *VCMsh2^{LoxP/null}* mice developed 1.40±0.11 intestinal tumors, the *VCMsh2^{LoxP/G674D}* mice developed 3.43±0.42 tumors (p<0.0001). There was also a significant difference in tumor size. Tumors in *VCMsh2^{LoxP/null}* mice had an average diameter of 6.48±0.58 mm, while the tumors in *VCMsh2^{LoxP/G674D}* mice were significantly smaller with a size of 3.25±0.49 mm (P<0.003). In *VCMsh2^{LoxP/null}* mice 18% (3/17) of the intestinal tumors were

adenomas and 82% (14/17) of tumors had progressed to adenocarcinoma. In *VCMsh2^{LoxP/G674D}* mice 37% (7/19) of intestinal tumors were adenomas, while 63% (12/19) were adenocarcinomas.

***VCMsh2^{LoxP/null}* and *VCMsh2^{LoxP/G674D}* Response to Cisplatin and FOLFOX**

Allelic phase mutant mice were subjected to chemotherapy with either cisplatin or FOLFOX, and tumor response was analyzed by MRI (Fig. 4C). Tumors in both *VCMsh2^{LoxP/null}* and *VCMsh2^{LoxP/G674D}* mice continued growing after receiving Phosphate Buffered Saline (PBS) injections (i.p.). The two groups, however, differed in response to cisplatin or FOLFOX treatment. *VCMsh2^{LoxP/null}* tumors were predominantly resistant to both chemotherapies, and only a small number of tumors showed growth retardation. In contrast almost all tumors in *VCMsh2^{LoxP/G674D}* mice responded well to either cisplatin or FOLFOX treatment regimen (Fig. 5).

To determine the molecular basis underlying the differences in intestinal tumorigenesis and drug response in *VCMsh2^{LoxP/null}* and *VCMsh2^{LoxP/G674D}* mice we performed *in vivo* analyses of MMR and the DNA damage response in the intestinal epithelium. While genomic DNA in the intestinal mucosa of wild type mice was previously shown to contain 4% unstable alleles at the dinucleotide marker D7Mit91²¹, genomic DNA in the mucosa of *VCMsh2^{LoxP/null}* and *VCMsh2^{LoxP/G674D}* mice displayed a significant increase in MSI at this marker that was comparable between both mouse lines (26/81 (32%) unstable alleles in *VCMsh2^{LoxP/null}* mice; 30/89 (31%) unstable alleles in *VCMsh2^{LoxP/G674D}* mice).

To determine whether *VCMsh2^{LoxP/G674D}* mice sustain the MMR-dependent DNA damage response function post chemotherapy, the number of apoptotic cells in intestinal crypts was analyzed 18 hours after FOLFOX injection (Fig. 6). These measurements showed a significant reduction in the apoptotic response in *VCMsh2^{LoxP/null}* mice as compared to *Msh2^{LoxP/LoxP}* (wild-type) mice ($p < 0.001$). Although the apoptotic response in the mucosal epithelium of *VCMsh2^{LoxP/G674D}* mice was somewhat reduced in comparison to wild type mice, it was significantly higher than in *VCMsh2^{LoxP/null}* mice ($p = 0.0118$). As expected the apoptotic response appeared normal in the spleen in all three groups of mice ($p = 0.2929$). Overall, these studies indicate that although the intestinal epithelial cells in *VCMsh2^{LoxP/G674D}* mice display only a partial DNA damage response, it is still sufficient to significantly impact tumor growth after FOLFOX treatment.

Conclusions

We have generated a conditional *Msh2^{LoxP}* knockout allele in mice that permits better modeling of the intestinal cancer features of Lynch Syndrome than previous models. Although these earlier mouse models are prone to a variety of cancers, they predominantly develop aggressive lymphomas early in life which has limited their use as preclinical models⁴⁻⁶. Using the *Msh2^{LoxP}* allele in combination with the *Villin-Cre* transgene we show that the lymphoma phenotype of constitutional *Msh2* knockout mice can be avoided and tumorigenesis restricted to the intestinal tract.

VCMsh2^{LoxP/LoxP} intestinal tissues display a high degree of MSI and tumors carry *Apc* mutations. A few documented Lynch Syndrome families exist with biallelic mutations in MMR genes²²⁻²⁴. These patients display severe reduction in life span and hematological malignancies, a phenotype that resembles neurofibromatosis, as well as CRCs. Since MSI can also be found in many solid tumors²⁵, the *Msh2^{LoxP}* allele should be helpful in modeling these types of MSI positive cancers. We have found, for instance, that the *Msh2^{LoxP}* allele in combination with the *Cre* transgene under control of the human epithelial keratin 14 promoter (*K14-cre*) permits the generation of skin tumors (data not shown). The

identification of tissue specific pathways altered in these tumors may be useful in identifying tissue specific cancer genes.

Similar to other mouse models of colorectal cancer, *VCMsh2^{LoxP/LoxP}* mice develop tumors predominantly in the small intestine, in contrast to Lynch Syndrome patients who typically develop tumors of the colon. Inactivation of an *Apc^{LoxP}* allele by *Villin-cre* also resulted mainly in small intestinal tumors. However, the tumor location could be shifted to the large intestine by colonic infection of *Apc^{LoxP/LoxP}* mice with Adenoviral-Cre (personal communication, Dr. Kenneth Hung). We are currently infecting the intestines of *Msh2^{LoxP/LoxP}* mice with *Adenoviral-Cre* to determine if this method may also be useful in permitting development of CRC without prior mutation to the *Apc* gene. Genetic approaches may also be useful in these experiments such as the introduction of retinoblastoma deficiency into *Msh2^{LoxP/LoxP}* mice, followed by infection with *Adenoviral-Cre*. While *Rb* deficiency by itself does not cause CRC²⁶, it has been demonstrated to expand the compartment that tumors occur in to include the cecum and distal colon in *Apc* deficient mice²⁷. We also combined the *Msh2^{LoxP}* allele with the *Cdx2P-NLS-Cre* transgene²⁸ and observed a shift of tumors to the large intestine. However, like *Msh2^{null}* mice, these animals also developed lymphomas (Kyeryoung Lee and Winfried Edelmann, unpublished observations).

Despite the tumor location in the small intestine, *VCMsh2^{LoxP}* mice have been highly useful in determining the effect of different *Msh2* alleles on intestinal tumorigenesis. In this study, we introduced either an *Msh2^{null}* knockout allele that causes complete loss of MSH2, or the *Msh2^{G674D}* allele representing a Lynch Syndrome missense mutation into *VCMsh2^{LoxP}* mice. Interestingly, *VCMsh2^{LoxP/G674D}* mice developed a higher number of intestinal tumors. However, the tumors developed at a later age and their size was reduced compared to *VCMsh2^{LoxP/null}* mice. It is possible that the accelerated tumorigenesis and larger tumor size in *VCMsh2^{LoxP/null}* mice led to intestinal obstruction and early death, preventing higher tumor multiplicity later in life. These data indicate that *Msh2* missense mutations can have distinct effects on intestinal tumorigenesis.

The *Msh2^{G674D}* mutation is located within the MSH2 ATPase domain at the identical amino acid residue as the *Msh2^{G674A}* mutation previously studied²⁹. Neither mutation affect the DNA damage response function, and *in vitro* analysis using *Msh2^{G674D/G674D}* MEFs showed a normal apoptotic response to FOLFOX exposure as did MEFs from wildtype mice. *Msh2^{-/-}* MEFs displayed increased resistance (data not shown). Our *in vivo* analysis further showed that the *Msh2^{G674D}* mutation caused complete MMR deficiency in the intestinal mucosa of *VCMsh2^{LoxP/G674D}* mice but left the MMR-dependent DNA damage response function partially intact. These results support the idea that the DNA damage response function of MMR is important for the suppression of the early steps of intestinal tumorigenesis³⁰.

Retention of the DNA damage response function in *VCMsh2^{G674D}* mice also had a significant impact on tumor response to chemotherapy. MRI based *in vivo* measurements of tumor growth showed that the intestinal tumors in *VCMsh2^{LoxP/G674D}* animals were sensitive to both cisplatin and FOLFOX, while tumors from *VCMsh2^{LoxP/null}* mice were generally resistant to both drugs. While cisplatin is commonly used to treat solid tumors³¹ and sometimes GI tumors in combination treatment regimen (esophagus, stomach, anus, and sometimes small intestine), it is not routinely used to treat CRC. It is a platinum based drug that introduces GpG cross-links into DNA. These lesions are recognized by MutS α with high specificity; and MSH2-deficient cells display low level resistance to the drug^{32, 33}. *In vitro*, MutS α binds to cross links, recruits MutL α , and interacts with the helicase domain of FANCI (Fanconi Anemia protein) for cross link repair. The response of *VCMsh2^{LoxP/null}*

and *VCMsh2^{LoxP/G674D}* tumors to cisplatin is consistent with the notion that complete loss of MSH2 diminishes cross link repair, and that less severe mutations might still be able to recruit repair factors for the removal of such lesions.

FOLFOX (5-fluorouracil (5-FU), leucovorin, and oxaliplatin) is commonly used for the treatment of late stage colorectal cancers. 5-FU-based adjuvant chemotherapy benefits patients with MSS tumors, but not patients with MSI positive tumors³⁴. Our finding that *VCMsh2^{LoxP/null}* tumors are resistant to FOLFOX is consistent with these studies. There is significant *in vitro* evidence that MMR defective colon cancer cell lines are resistant to killing by 5-FU, and that re-expression of MMR genes in these cell lines reverses the phenotype^{35, 36}. 5-FU acts to disrupt RNA synthesis and inactivate thymidylate synthase. It is also incorporated into DNA, and therefore could be processed by MMR. 5-FU substrates are recognized by MutSa, suggesting CRC chemosensitivity may in part be due to MMR protein recognition, leading to cell death either by futile repair cycles or signaling of cell cycle arrest and apoptosis³⁷. *VCMsh2^{LoxP/G674D}* tumor sensitivity to FOLFOX implies that MutSa complexes interact with 5-FU adducts and mediate a cytotoxic response. It also raises the possibility that some tumors in human patients carrying *MSH2* missense mutations that cause MSI without affecting DNA damage response will remain responsive to fluorouracil-based adjuvant chemotherapy.

Supplementary Material

Refer to Web version on PubMed Central for supplementary material.

Acknowledgments

We would like to thank Larissa Georgeon Richard for E-cadherin IHC on *VCMsh2^{LoxP/LoxP}* adenocarcinomas and Dr. Kenneth Hung for discussions of work with *Adenoviral-Cre* on *Apc* conditional knockout mice.

Grant support: This work was supported by NIH Grants ES11040 (R.K.) CA084301 (R.K.) and CA76329 (W.E.) and CA93484 (W.E.). Center grant CA13330 (Albert Einstein College of Medicine), Project Z01 ES065089, Division of Intramural Research of the NIH, NIEHS (T.A.K.).

References

1. Fishel R, Lescoe MK, Rao MR, et al. The human mutator gene homolog MSH2 and its association with hereditary nonpolyposis colon cancer. *Cell* 1993;75:1027–38. [PubMed: 8252616]
2. Lothe RA, Peltomaki P, Meling GI, et al. Genomic instability in colorectal cancer: relationship to clinicopathological variables and family history. *Cancer Res* 1993;53:5849–52. [PubMed: 8261392]
3. Marsischky GT, Filosi N, Kane MF, et al. Redundancy of *Saccharomyces cerevisiae* MSH3 and MSH6 in MSH2-dependent mismatch repair. *Genes Dev* 1996;10:407–20. [PubMed: 8600025]
4. de Wind N, Dekker M, Berns A, et al. Inactivation of the mouse Msh2 gene results in mismatch repair deficiency, methylation tolerance, hyperrecombination, and predisposition to cancer. *Cell* 1995;82:321–30. [PubMed: 7628020]
5. Reitmair AH, Schmits R, Ewel A, et al. MSH2 deficient mice are viable and susceptible to lymphoid tumours. *Nat Genet* 1995;11:64–70. [PubMed: 7550317]
6. Smits R, Hofland N, Edelmann W, et al. Somatic *Apc* mutations are selected upon their capacity to inactivate the beta-catenin downregulating activity. *Genes Chromosomes Cancer* 2000;29:229–39. [PubMed: 10992298]
7. Reitmair AH, Cai JC, Bjerknes M, et al. MSH2 deficiency contributes to accelerated APC-mediated intestinal tumorigenesis. *Cancer Res* 1996;56:2922–6. [PubMed: 8674041]
8. Lee EC, Yu D, Martinez de Velasco J, et al. A highly efficient *Escherichia coli*-based chromosome engineering system adapted for recombinogenic targeting and subcloning of BAC DNA. *Genomics* 2001;73:56–65. [PubMed: 11352566]

9. Liu P, Jenkins NA, Copeland NG. A highly efficient recombineering-based method for generating conditional knockout mutations. *Genome Res* 2003;13:476–84. [PubMed: 12618378]
10. Ioffe E, Liu Y, Bhaumik M, et al. WW6: an embryonic stem cell line with an inert genetic marker that can be traced in chimeras. *Proc Natl Acad Sci U S A* 1995;92:7357–61. [PubMed: 7638196]
11. Rodriguez CI, Buchholz F, Galloway J, et al. High-efficiency deleter mice show that FLPe is an alternative to Cre-loxP. *Nat Genet* 2000;25:139–40. [PubMed: 10835623]
12. Lakso M, Pichel JG, Gorman JR, et al. Efficient in vivo manipulation of mouse genomic sequences at the zygote stage. *Proc Natl Acad Sci U S A* 1996;93:5860–5. [PubMed: 8650183]
13. el Marjou F, Janssen KP, Chang BH, et al. Tissue-specific and inducible Cre-mediated recombination in the gut epithelium. *Genesis* 2004;39:186–93. [PubMed: 15282745]
14. Thomas DC, Umar A, Kunkel TA. Measurement of heteroduplex repair in human cell extracts. *Methods: A companion to Methods in Enzymology* 1995;7:187–197.
15. Thomas DC, Roberts JD, Kunkel TA. Heteroduplex repair in extracts of human HeLa cells. *J Biol Chem* 1991;266:3744–51. [PubMed: 1995629]
16. Kabbarah O, Mallon MA, Pfeifer JD, et al. A panel of repeat markers for detection of microsatellite instability in murine tumors. *Mol Carcinog* 2003;38:155–9. [PubMed: 14639654]
17. Dietrich WF, Miller JC, Steen RG, et al. A genetic map of the mouse with 4,006 simple sequence length polymorphisms. *Nat Genet* 1994;7:220–45. [PubMed: 7920646]
18. Kuraguchi M, Edelmann W, Yang K, et al. Tumor-associated Apc mutations in Mlh1^{-/-} Apc^{1638N} mice reveal a mutational signature of Mlh1 deficiency. *Oncogene* 2000;19:5755–63. [PubMed: 11126362]
19. Wei K, Clark AB, Wong E, et al. Inactivation of Exonuclease 1 in mice results in DNA mismatch repair defects, increased cancer susceptibility, and male and female sterility. *Genes Dev* 2003;17:603–14. [PubMed: 12629043]
20. Andreutti-Zaugg C, Scott RJ, Iggo R. Inhibition of nonsense-mediated messenger RNA decay in clinical samples facilitates detection of human MSH2 mutations with an in vivo fusion protein assay and conventional techniques. *Cancer Res* 1997;57:3288–93. [PubMed: 9242462]
21. Avdievich E, Reiss C, Scherer SJ, et al. Distinct effects of the recurrent Mlh1G67R mutation on MMR functions, cancer, and meiosis. *Proc Natl Acad Sci U S A* 2008;105:4247–52. [PubMed: 18337503]
22. Menko FH, Kaspers GL, Meijer GA, et al. A homozygous MSH6 mutation in a child with cafe-au-lait spots, oligodendroglioma and rectal cancer. *Fam Cancer* 2004;3:123–7. [PubMed: 15340263]
23. Rævaara TE, Gerdes AM, Lonnqvist KE, et al. HNPCC mutation MLH1 P648S makes the functional protein unstable, and homozygosity predisposes to mild neurofibromatosis type 1. *Genes Chromosomes Cancer* 2004;40:261–5. [PubMed: 15139004]
24. Rey JM, Noruzinia M, Brouillet JP, et al. Six novel heterozygous MLH1, MSH2, and MSH6 and one homozygous MLH1 germline mutations in hereditary nonpolyposis colorectal cancer. *Cancer Genet Cytogenet* 2004;155:149–51. [PubMed: 15571801]
25. Boland CR, Thibodeau SN, Hamilton SR, et al. A National Cancer Institute Workshop on Microsatellite Instability for cancer detection and familial predisposition: development of international criteria for the determination of microsatellite instability in colorectal cancer. *Cancer Res* 1998;58:5248–57. [PubMed: 9823339]
26. Kucherlapati MH, Nguyen AA, Bronson RT, et al. Inactivation of conditional Rb by Villin-Cre leads to aggressive tumors outside the gastrointestinal tract. *Cancer Res* 2006;66:3576–83. [PubMed: 16585182]
27. Kucherlapati MH, Yang K, Fan K, et al. Loss of Rb1 in the gastrointestinal tract of Apc^{1638N} mice promotes tumors of the cecum and proximal colon. *Proc Natl Acad Sci U S A* 2008;105:15493–8. [PubMed: 18832169]
28. Hinoi T, Akyol A, Theisen BK, et al. Mouse model of colonic adenoma-carcinoma progression based on somatic Apc inactivation. *Cancer Res* 2007;67:9721–30. [PubMed: 17942902]
29. Lin DP, Wang Y, Scherer SJ, et al. An Msh2 point mutation uncouples DNA mismatch repair and apoptosis. *Cancer Res* 2004;64:517–22. [PubMed: 14744764]
30. Fishel R. The selection for mismatch repair defects in hereditary nonpolyposis colorectal cancer: revising the mutator hypothesis. *Cancer Res* 2001;61:7369–74. [PubMed: 11606363]

31. Siddik ZH. Cisplatin: mode of cytotoxic action and molecular basis of resistance. *Oncogene* 2003;22:7265–79. [PubMed: 14576837]
32. Yamada M, O'Regan E, Brown R, et al. Selective recognition of a cisplatin-DNA adduct by human mismatch repair proteins. *Nucleic Acids Res* 1997;25:491–6. [PubMed: 9016586]
33. Stojic L, Brun R, Jiricny J. Mismatch repair and DNA damage signalling. *DNA Repair (Amst)* 2004;3:1091–101. [PubMed: 15279797]
34. Ribic CM, Sargent DJ, Moore MJ, et al. Tumor microsatellite-instability status as a predictor of benefit from fluorouracil-based adjuvant chemotherapy for colon cancer. *N Engl J Med* 2003;349:247–57. [PubMed: 12867608]
35. Carethers JM, Chauhan DP, Fink D, et al. Mismatch repair proficiency and in vitro response to 5-fluorouracil. *Gastroenterology* 1999;117:123–31. [PubMed: 10381918]
36. Meyers M, Wagner MW, Hwang HS, et al. Role of the hMLH1 DNA mismatch repair protein in fluoropyrimidine-mediated cell death and cell cycle responses. *Cancer Res* 2001;61:5193–201. [PubMed: 11431359]
37. Tajima A, Hess MT, Cabrera BL, et al. The mismatch repair complex hMutS alpha recognizes 5-fluorouracil-modified DNA: implications for chemosensitivity and resistance. *Gastroenterology* 2004;127:1678–84. [PubMed: 15578504]

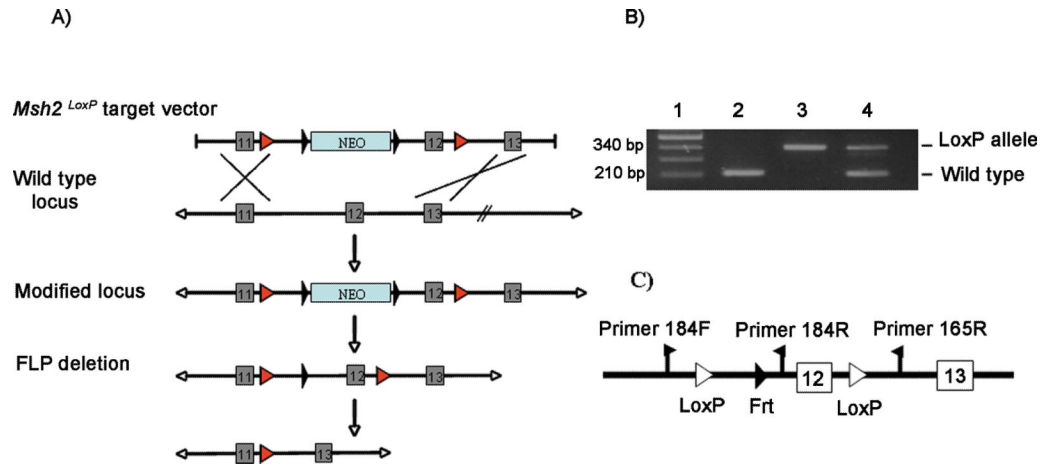
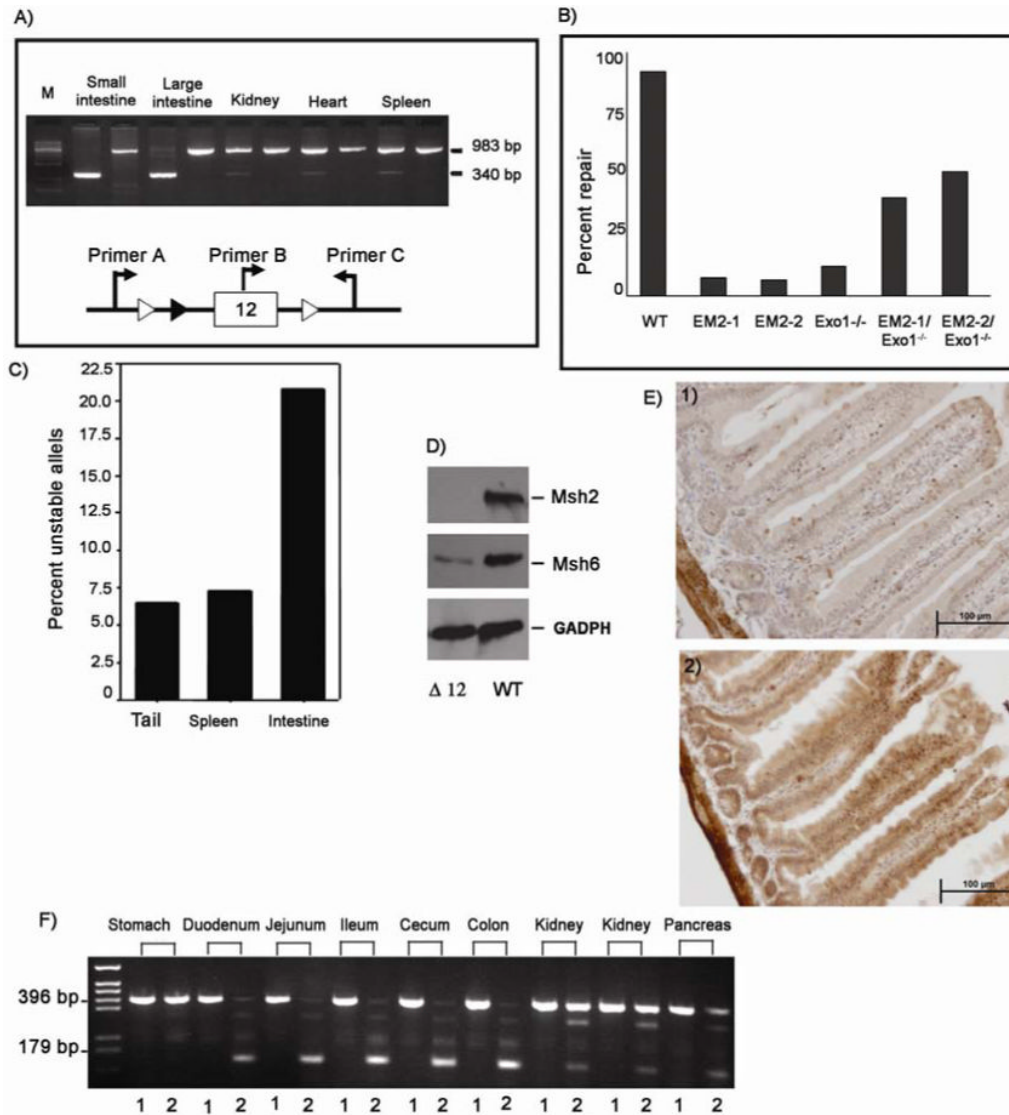


Figure 1.

Strategy for the production of *Msh2* conditional knockout mutant mice, and PCR genotyping of offspring. (A) Gene targeting strategy. (B) PCR genotyping strategy. 1) pGEM markers, 2) Wildtype mouse, 3) *Msh2*^{LoxP/LoxP}, exon 12 deleted, 4) *Msh2*^{LoxP/+}. (C) Where *Msh2* exon 12 has been deleted, primer pair 184F/184R amplifies no product, whereas primer pair 184F/165R amplifies a 340 bp product. Wildtype animals without the conditional allele amplify a 210 bp PCR product using primers 184F/184R.

**Figure 2.**

Molecular characterization of *VCMsh2^{LoxP/LoxP}* and *ECMsh2^{LoxP/LoxP}* mice. (A) Specific rearrangement of the *Msh2* gene in the small and large intestines of *VCMsh2^{LoxP/LoxP}* animals, is absent in the kidney heart and spleen. Primer pairs A/C amplify a 340 bp product when exon 12 is deleted (intestine) and a 983 bp product when exon 12 is intact (kidney heart and spleen). (B) Measurement of MMR in *ECMsh2^{LoxP/LoxP}* MEFs. Cell lines EM2-1 and EM2-2 are MMR deficient and compare to the *Exo1^{-/-}* MMR deficient cell line, EM2 and *Exo1^{-/-}* cell lines complement each other. (C) MSI in *VCMsh2^{LoxP/LoxP}* mice (for MSI in C57B1/6J mice see 19). (D) Western blot analysis of EM2 MEF cell lines. (Δ12), MSH2 is absent from an EM2 cell line and shows reduced amounts of its complex partner, Msh6. WT, wildtype mouse embryonic fibroblast cell line. (E) IHC on *VCMsh2^{LoxP/LoxP}* small intestine (top) compared to wildtype intestine (bottom). (F) RT-PCR using *Msh2* primers with GI tissues 1) wildtype, 2) *VCMsh2^{LoxP/LoxP}*.

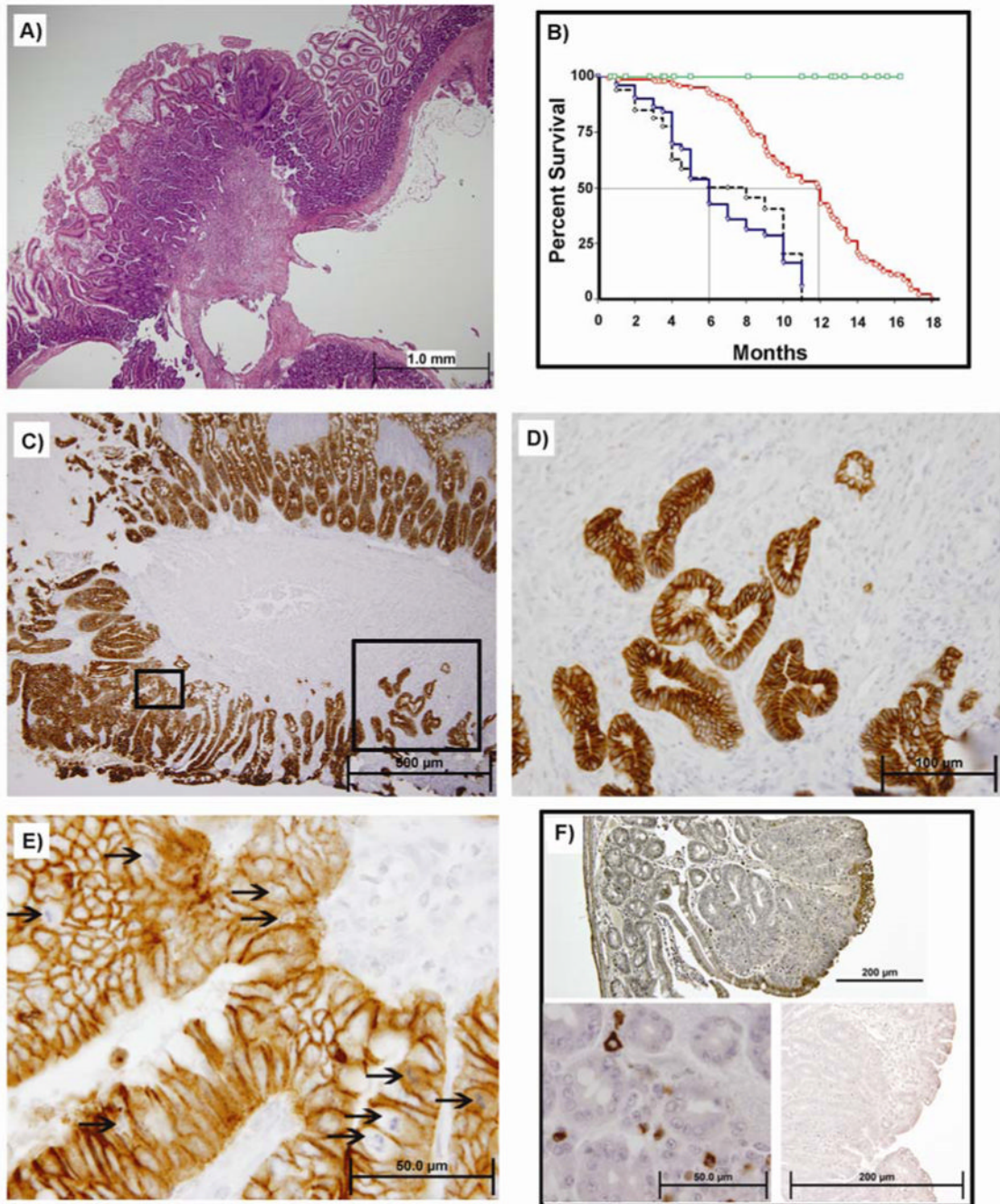


Figure 3.

VCMsh2^{LoxP/LoxP} mice have decreased median survival. (A) An intestinal adenocarcinoma from a *VCMsh2^{LoxP/LoxP}* mouse. (B) Survival curves: wildtype, (green); *VCMsh2^{LoxP/LoxP}*, (red); *ECMsh2^{LoxP/LoxP}*, (blue, solid); *Msh2^{null}* (black, dashed). (C) An intestinal adenocarcinoma from a *VCMsh2^{LoxP/LoxP}* mouse stained with rabbit anti mouse E cadherin -24E10 (Cell Signaling Technology, Danvers, MA). The black square on the lower right shows tumor invasion of the muscularis and is enlarged in panel D). The smaller square on the lower right is enlarged in panel E) and shows multiple mitotic figures indicated by black arrows. F) IHC using antibody to *Apc* on a *VCMsh2^{LoxP/LoxP}* intestinal polyp (top), specific

staining of *Apc* in macrophages of the intestinal epithelium (lower left), wildtype control (lower right).

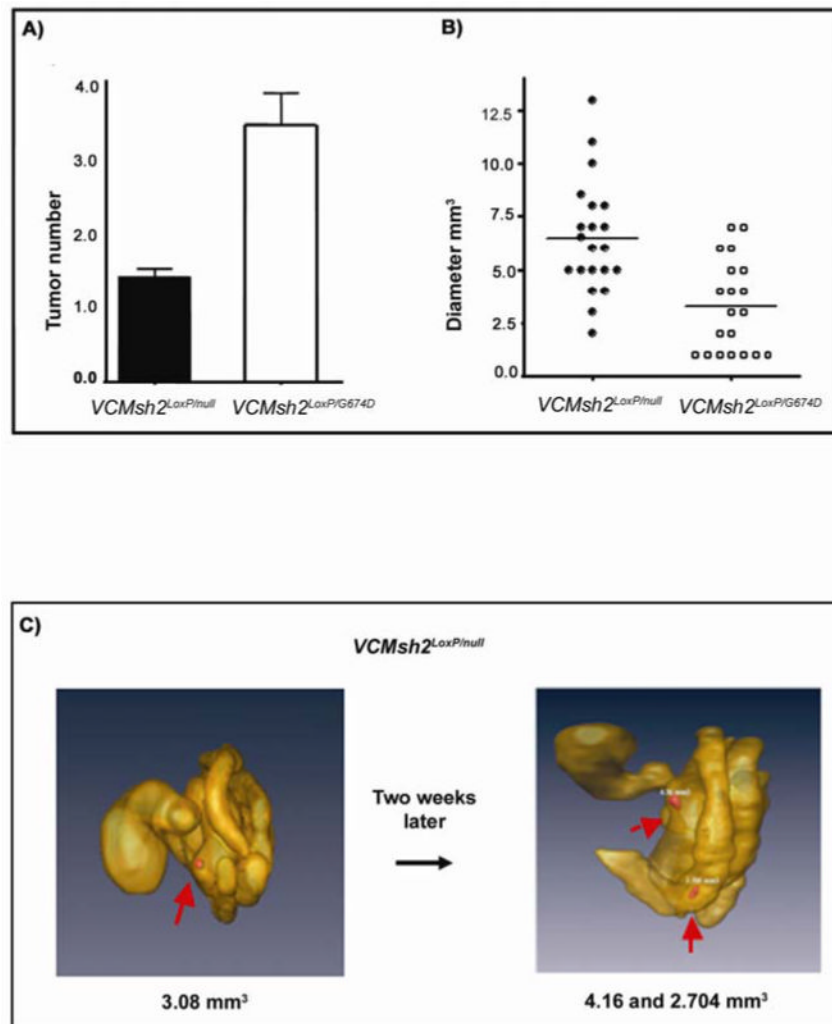


Figure 4. Tumor size measurements by caliper and tumor number count, from the intestines of allelic phase mutants. (A) The average number of tumors between *VCMsh2^{LoxP/Inull}* and *VCMsh2^{LoxP/G674D}* mice varied significantly, as did the size (B). (C) Intestinal tumors for chemotherapy are visualized and measured by MRI. A six month old *VCMsh2^{LoxP}* mouse testing positive for occult blood, was subjected to MRI, successfully revealing one tumor. Two weeks later a second tumor was detected during a second MRI at the original location.

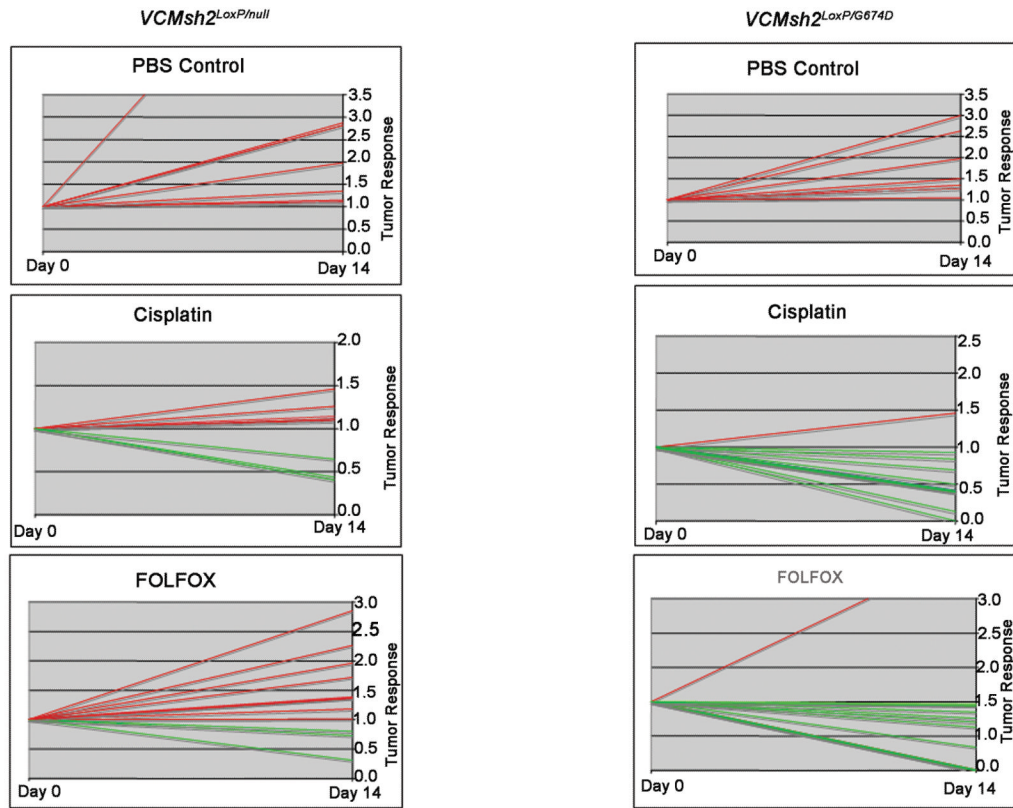


Figure 5. Intestinal tumors from *VCMsh2^{LoxP/null}* and *VCMsh2^{LoxP/G674D}* mice, respond to chemotherapy. Tumors are measured in terms of relativity of MRI measurements. The tumor size at day 0 is 1, and the relative tumor growth or retardation is scored on the basis of percentage. Red lines indicate growth, green lines indicate retardation. The number of tumors for each treatment is as follows. *VCMsh2^{LoxP/null}*: PBS-7, cisplatin-8, FOLFOX-11. For *VCMsh2^{LoxP/G674D}*: PBS-7, cisplatin-9, FOLFOX-11.

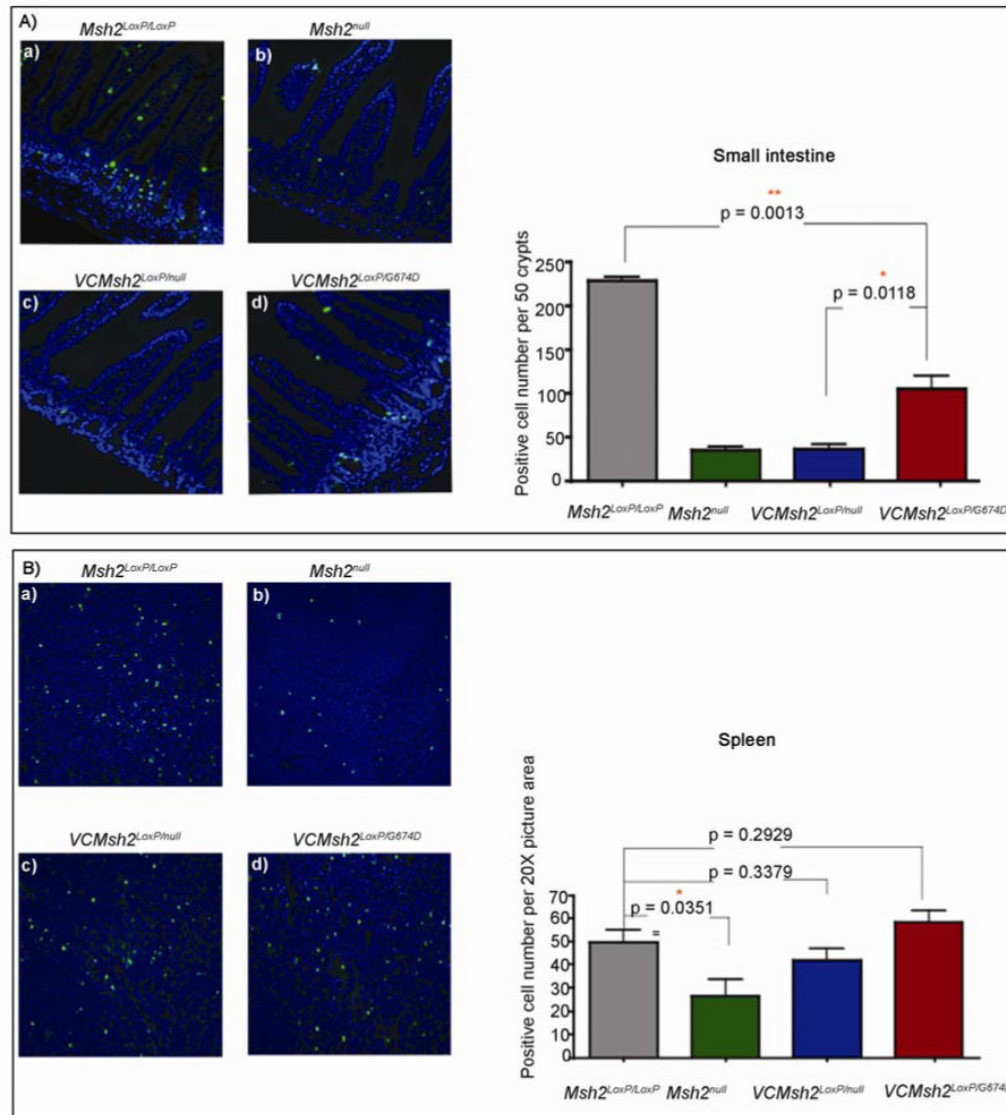


Figure 6. Apoptosis measured in intestinal mucosa of *VCMsh2*^{LoxP/null} and *VCMsh2*^{LoxP/G674D} mice, after 18 hours of FOLFOX treatment. (A) TUNEL staining (green fluorescence) in the intestinal mucosa of a. *Msh2*^{LoxP/LoxP}, b. *Msh2*^{null}, c. *VCMsh2*^{LoxP/null}, d. *VCMsh2*^{LoxP/G674D} mice with graphic analysis of the number of positive apoptotic cells per fifty crypts. (B) Apoptosis measured in the spleen of *VCMsh2*^{LoxP/null} and *VCMsh2*^{LoxP/G674D} mice, after 18 hours of FOLFOX treatment. A. TUNEL staining (green fluorescence) in the intestinal mucosa of a. *Msh2*^{LoxP/LoxP}, b. *Msh2*^{null}, c. *VCMsh2*^{LoxP/null}, d. *VCMsh2*^{LoxP/G674D} mice with graphic analysis of the number of positive apoptotic cells per fifty crypts.

Table 1

***VCMSH2^{LoxP/LoxP}* Tumor Incidence and Multiplicity**

Genotype	N	Age (mo) Mean ± SD	Sex (M:F)	Overall	Intestinal tumors n (%)		Intestinal Tumor Multiplicity (Mean ± SEM)
					Lymphoma	Intestine	
<i>VCMSH2^{LoxP/LoxP}</i>	18	9.0 ± 1.1	1:0.8	16 (89) ^b	0 (0)	16 (89) ^b	1.61 ± 0.30 ^c
<i>VCMSH2^{LoxP/+}</i>	15	11.3 ± 1.8	1:1.5	0 (0) ^b	0 (0)	0 (0) ^b	0.00 ± 0.00 ^c
<i>Msh2^{+/+}</i>	17	14.2 ± 2.7	1:0.4	1 (6) ^b	0 (0)	1 (6) ^b	0.06 ± 0.00 ^c

N, number of mice studied; n, number of mice with intestinal tumors.

^a*Msh2^{+/+}* mice, VC positive and VC negative combined.

^bTumor incidence compared by Fisher exact probability: P<0.0001.

^cTumor multiplicity compared by Mann-Whitney or binomial calculation: P<0.0001.

Table 2
Truncation mutations to *Apc* in tumors from *VCMsh2^{LoxP/LoxP}*

Codon	Mutation	Consequence	WT sequence	Mutations found
684	del A	frameshift	TTG TGG AAT CTC	2
874	C to T	Arg to Stop	TCA AAA CGA GGT	1
854	C to T	Arg to Stop	AGA GAG CGA GGT	2
957	C to T	Arg to Stop	TAT AAA CGA TCT	1
1098	del T	frameshift	GAA TGT GTT TCC CCA	1
1211	del TC	frameshift	CAT CTC TCT CCA AGC	2
1464	del AG	frameshift	AGA GAG AGT GGG	1